European Journal of Medicinal Chemistry 217 (2021) 113339

Contents lists available at ScienceDirect

European Journal of Medicinal Chemistry

journal homepage: http://www.elsevier.com/locate/ejmech

Synthesis, biological evaluation, and docking studies of novel pyrrolo[2,3-*b*]pyridine derivatives as both ectonucleotide pyrophosphatase/phosphodiesterase inhibitors and antiproliferative agents

Saif Ullah [a], Mohammed I. El-Gamal [b, c, d, 1], Randa El-Gamal [e], Julie Pelletier [f], Jean Sévigny [f, g], Mahmoud K. Shehata [c], Hanan S. Anbar [h, *], Jamshed Iqbal [a, **]

[a] Centre for Advanced Drug Research, COMSATS University Islamabad, Abbottabad Campus, Abbottabad, 22060, Pakistan
[b] Department of Medicinal Chemistry, College of Pharmacy, University of Sharjah, Sharjah, 27272, United Arab Emirates
[c] Sharjah Institute for Medical Research, University of Sharjah, Sharjah, 27272, United Arab Emirates
[d] Department of Medicinal Chemistry, Faculty of Pharmacy, University of Mansoura, Mansoura, 35516, Egypt
[e] Department of Medical Biochemistry, Faculty of Medicine, University of Mansoura, Mansoura, 35516, Egypt
[f] Centre de Recherche du CHU de Québec – Université Laval, Québec, QC, G1V 4G2, Canada
[g] Département de microbiologie-infectiologie et d'immunologie, Faculté de Médecine, Université Laval, Québec, QC, G1V 0A6, Canada
[h] Department of Clinical Pharmacy and Pharmacotherapeutics, Dubai Pharmacy College for Girls, Dubai, 19099, United Arab Emirates

ARTICLE INFO

Article history:
Received 4 January 2021
Received in revised form
25 February 2021
Accepted 26 February 2021
Available online 10 March 2021

Keywords:
Antiproliferative activity
Molecular docking studies
NPP1 and NPP3
Pyrrolo[2,3-*b*]pyridine scaffold
Sulfonylurea

ABSTRACT

Ecto-nucleotide pyrophosphatases/phosphodiesterases (NPPs) together with nucleoside triphosphate diphosphohydrolases (NTPDases) and alkaline phosphatases (APs) are nucleotidases located at the surface of the cells. NPP1 and NPP3 are important members of NPP family that are known as druggable targets for a number of disorders such as impaired calcification, type 2 diabetes, and cancer. Sulfonylurea derivatives have been reported as antidiabetic and anticancer agents, therefore, we synthesized and investigated series of sulfonylurea derivatives **1a-m** possessing pyrrolo[2,3-*b*]pyridine core as inhibitors of NPP1 and NPP3 isozymes that are over-expressed in cancer and diabetes. The enzymatic evaluation highlighted compound **1a** as selective NPP1 inhibitor, however, **1c** was observed as the most potent inhibitor of NPP1 with an IC_{50} value of 0.80 ± 0.04 μM. Compound **1l** was found to be the most potent and moderately selective inhibitor of NPP3 (IC_{50} = 0.55 ± 0.01 μM). Furthermore, *in vitro* cytotoxicity assays of compounds **1a-m** against MCF-7 and HT-29 cancer cell lines exhibited compound **1c** (IC_{50} = 4.70 ± 0.67 μM), and **1h** (IC_{50} = 1.58 ± 0.20 μM) as the most cytotoxic compounds against MCF-7 and HT-29 cancer cell lines, respectively. Both of the investigated compounds showed high degree of selectivity towards cancer cells than normal cells (WI-38). Molecular docking studies of selective and potent enzyme inhibitors revealed promising mode of interactions with important binding sites residues of both isozymes i.e., Thr256, His380, Lys255, Asn277 residues of NPP1 and His329, Thr205, and Leu239 residues of NPP3. In addition, the most potent antiproliferative agent, compound **1h**, doesn't produce hypoglycemia as a side effect when injected to mice. This is an additional merit of the promising compound **1h**.

1. Introduction

The prominent ectonucleotidases involved in the hydrolysis of extracellularly located nucleotidases are ectonucleotide pyrophosphatase/phosphodiesterases (NPPs), and nucleoside triphosphate diphosphohydrolases (NTPDases) [1]. NPPs exist as membrane-bound glycoproteins (NPP1 & NPP3) and as soluble proteins (NPP2). The plasma membrane-bound proteins hydrolyze the terminal phosphate of nucleotides through an extracellularly located active site [2]. Both of NPP1 and NPP3 act on a wide range of substrates, involving adenosine triphosphate (ATP), adenosine diphosphate (ADP), phosphoadenylate sulfate, nucleotide-based

* Corresponding author.
** Corresponding author.
E-mail addresses: dr.hanan@dpc.edu (H.S. Anbar), drjamshed@cuiatd.edu.pk (J. Iqbal).
[1] Co-first author.

https://doi.org/10.1016/j.ejmech.2021.113339
0223-5234/

sugars (UDP-glucoside) and dinucleoside polyphosphates (AP3A, AP4A), to their respective nucleoside monophosphates [3,4].

Expression of NPP1 is found in adipose tissues, bone, heart, placenta, testes, and liver [5]. The physiological role of NPP1 appears in the mineralization of bone, and cell calcification of vascular smooth muscles [6]. Over-expression of NPP1 leads to hypermineralization disorders such as deposition of calcium pyrophosphate dihydrate (CPPD), and calcific aortic valve disease [7–10]. The overexpression of NPP1 leads to insulin resistance because of inhibition of tyrosine kinase activity of β-subunit of insulin receptor [11]. Elevated expression of NPP1 is reported in rat C6 glioma cells, human stem-like cells glioblastoma, and astrocytic brain tumor [12,13]. In a recent study on small hairpin RNA knockdown of NPP1 expression decreases the cell proliferation and forces the cell death [14].

The second important isozyme NPP3 is mainly expressed on basophils, mast cells, mucosal, and epithelial surfaces. The NPP3 expression is found to be up-regulated due to release of inflammatory mediators as a result of basophils activation by antigen-bound IgE antibody, therefore, NPP3 can act as diagnostic marker of allergen sensitivity [15,16]. Moreover, NPP3 is reported as tumor marker because its overexpression is involved in carcinogenesis and metastasis of tumor cells [8,17].

Pyrrolopyridine-based derivatives have widely been reported for their medicinal and therapeutic effects. A pyrrolopyridine derivative (BMS-911543) has been reported as potent inhibitor of Janus kinase 2 (JAK2) (compound **A**, Fig. 1) [18]. A condensed structure of pyrrolopyridine derivative was reported to be associated with lowering the level of JAK3 protein, acting as an important agent for the treatment or prevention of the diseases associated with undesirable cytokine signal transduction [19]. Another important derivative of pyrrolopyridine bearing pyradazinone core (*N*-(4-((1*H*-pyrrolo[2,3-*b*]pyridin-4-yl)oxy)phenyl)1-(4-chloro-3-(trifluoromethyl)phenyl)-4-oxo-1,4-dihydropyridazine-3-carboxamide) was reported as a potent inhibitor of c-Met kinase inhibitor (compound **B**, Fig. 1) [20]. A series of pyrrolopyridine derivatives showed significant affinity for cannabinoid receptors CB_1/CB_2 (compound **C**, Fig. 1) [21]. Moreover, a novel series of quinazoline-4-piperidine sulfamide analogues inhibited the hydrolytic activity of NPP1 with K_i value of 105 nM (compound **D**, Fig. 1) [22]. Also in our very recent study, we reported pyridine-pyrazole thioureas and pyridine-pyrazole sulfonamides as highly potent inhibitors of NPP1 and NPP3 with IC_{50} values of 0.18 μM, and 0.21 μM, respectively (compounds **E** and **F**, Fig. 1). These inhibitors of NPP1 and NPP3 also exhibited antiproliferative activity against different cancer cell lines [23].

Another well-known drug bearing the similar pharmacophore is Sulofenur (diarylsulfonylurea) that was reported as antiproliferative agent. However, it suffers from two drawbacks, first, it induces hypoglycemia as a side effect due to the presence of diarylurea scaffold. The second drawback is it causes hematological side effects due to formation of aniline derivative as a metabolite [24–26]. In our target compounds, they were designed to possess pyrrolopyridine nucleus as an attempt to avoid formation of aniline metabolite. In addition, the sulfonylurea linker was retained but embedded into the bicyclic ring (Fig. 1). The inhibitory effects of sulfonyl-possessing compounds (such as compounds **D-F**, Fig. 1) against NPP1 or NPP3 enzymes encouraged us to test our target

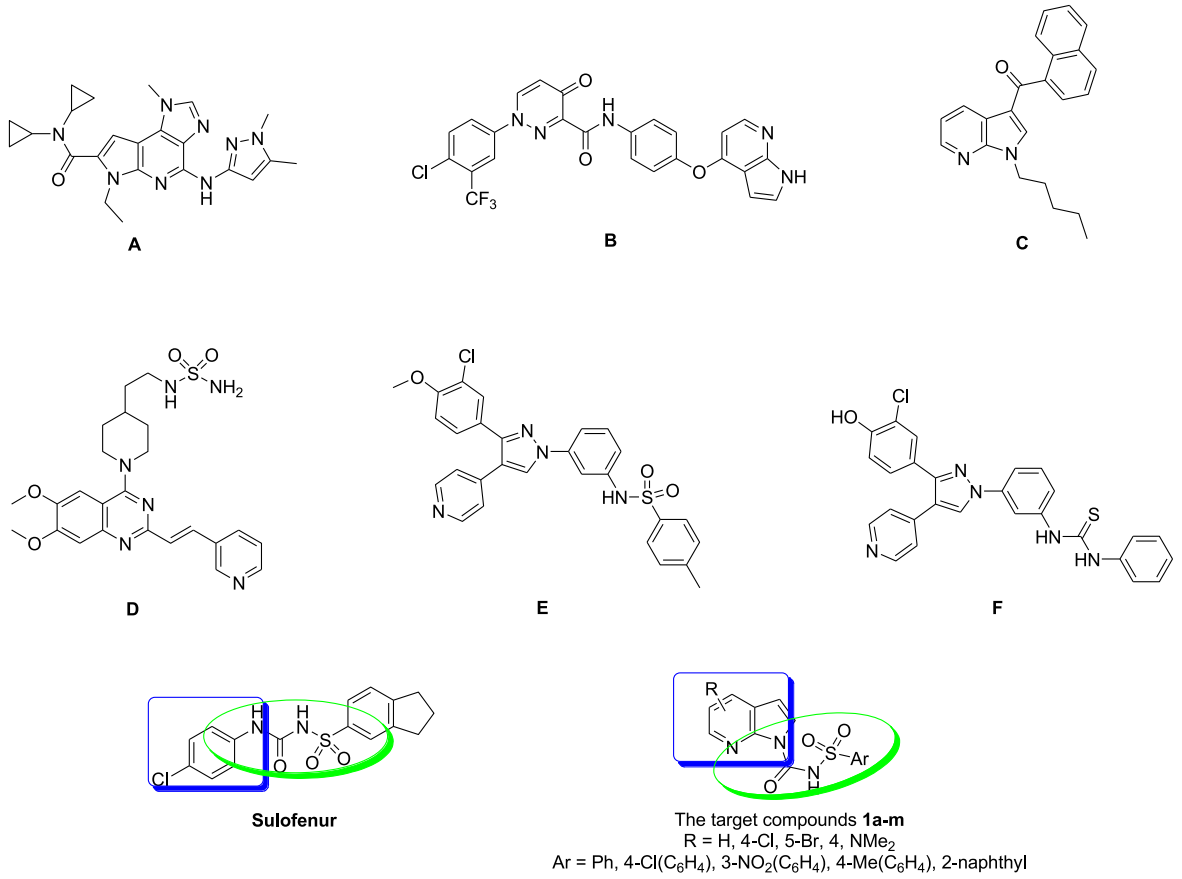

Fig. 1. Structures of reported therapeutically active pyrrolopyridine derivatives, sulfonyl/thiourea-based NPP inhibitors, and the target compounds **1a-m**.

compounds against NPP1 and NPP3. Moreover, investigation of the effect on blood glucose level was a part of our plans, hopefully, we can avoid this hypoglycemia issue that occurs with sulofenur.

Thus, considering the medicinal importance of fused pyrrolopyridine scaffold and sulfonamide (part of sulfonylurea moiety), we designed a series of novel structures possessing both pyrrolopyridine nucleus and sulfonylurea groups. We evaluated the newly synthesized compounds against NPP1 and NPP3 activity and their chemotherapeutic effects against cancer cell lines (MCF-7 and HT-29). Moreover, with the help of enzyme kinetics study we determined the mode of inhibition for compounds **1c** and **1l**.The molecular docking studies were performed to justify the putative binding mode of inhibitorswith amino acids residues for the most promising compounds. Furthermore, the most potent antiproliferative agent was tested for possible effect on blood sugar level in mice.

2. Results and discussion

2.1. Chemistry

We could successfully synthesize the target molecules **1a-m** *via* the synthetic pathway shown in Scheme 1. Upon reaction of arylsulfonyl chloride reagents **2a-e** with ammonium hydroxide (**3**), the corresponding aryl sulfonamides **4a-e** were formed [27]. On another side, fusion of 4-chloro-7-azaindole (**5c**) with dimethylammonium chloride at 180 °C for 5 h led to formation of 4-(dimethylamino)-7-azaindole (**7**) [28]. Interaction of compounds **5a-c** or **7** with phenyl chloroformate (**8**) in presence of triethylamine (TEA) produced the corresponding carbamate intermediates **9a-d**. In the final step, reaction of the synthesized sulfonamide reagents **4a-e** with carbamates **9a-d** in presence of potassium carbonate yielded the target sulfonylurea products **1a-m**.

2.2. Biological evaluation

2.2.1. Enzymatic assay for NPP1 and NPP3

The inhibitory effect of the target compounds on the activity of NPP1 and NPP3 was examined by using the already reported method with minor modifications [23,29]. The inhibitory potential of newly synthesized derivatives were measured by the decrease of the hydrolysis of an artificial substrate (thymidine 5′-monophosphate *para*-nitrophenyl ester (pNP-TMP)), as shown in Table 1.

2.2.1.1. Structure-activity relationship. Comparison of structure-activity relationship (SAR) of **1a**, **1f**, **1j**, and **1l** revealed that structural variation at position 4 at the pyrrolopyridine core with chlorine was much favorable for inhibition of isoenzyme NPP1 with an IC_{50} value of 1.08 ± 0.01 μM whereas, introduction of 4-dimethylamino group yielded compound **1l** that was considered among the active inhibitors of NPP3 (IC_{50} = 0.55 ± 0.01 μM). The simplest structure **1a** selectively inhibited the activity of NPP1 to an IC_{50} value of 4.50 ± 0.16 μM, and moderately affected the activity of NPP3 to only 37.5%. The SAR of **1a** and **1l** assumed that non-substituted or chloro-substituted structures were much tolerable for NPP1 inhibition. Introduction of chlorine at *para* position on benzenesulfonylurea moiety retained the activity towards NPP3 that was IC_{50} = 0.88 ± 0.01 μM, suggested that for inhibition of NPP3, chloro substitution was favorable at benzenesulfonylurea moiety instead of pyrrolopyridine core. SAR study of compound **1c** showed that presence of strong electron-withdrawing group (-NO_2) rendered the selectivity of **1c** and activity of NPP1 (IC_{50} = 0.80 ± 0.04 μM) *vs*. NPP3 which was moderately inhibited with an IC_{50} value of 1.17 ± 0.07 μM. The inhibitor **1g** with bromine at position 5 of pyrrolopyridine core, proved as dual inhibitor of both isoenzymes with moderate activity as compared to compound **1c**. On the contrary to **1b**, presence of electron-donating group (-CH_3) at *para* position of benzenesulfonylurea moiety (compound

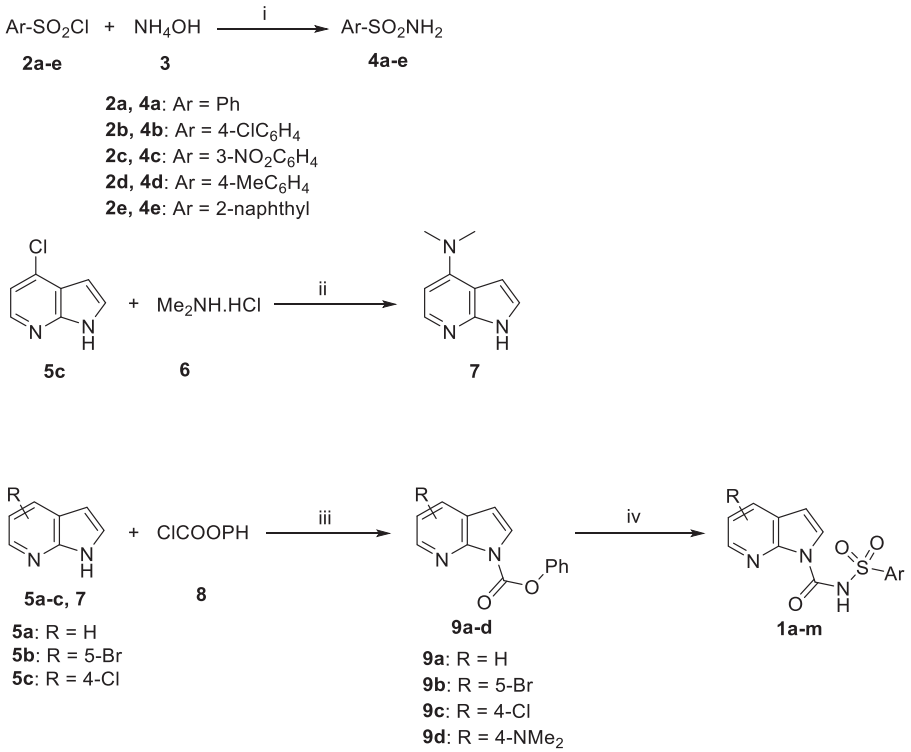

Scheme 1. Reagents and reaction conditions: (i) MeOH, rt, 5–10 min; (ii) 180 °C (fusion), 5 h; (iii) TEA, THF, 0 °C, 2 h; (iv) K_2CO_3, CH_2Cl_2, rt, overnight.

Table 1
Illustration of inhibitory potential of the compounds **1a-m** and suramin against NPP1 and NPP3 isozymes.

Compound No.	Chemical structure	IC_{50} ± S.E.M. in μM or % inhibition at 100 μM	
		NPP1	NPP3
1a	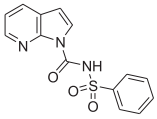	4.50 ± 0.16	37.5%
1b	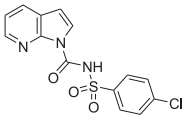	10.36 ± 0.03	0.88 ± 0.01
1c	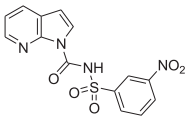	0.80 ± 0.04	1.17 ± 0.07
1d	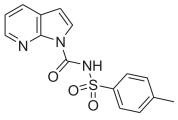	47.9%	3.72 ± 0.17
1e	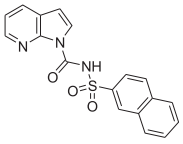	48.6%	44.1%
1f	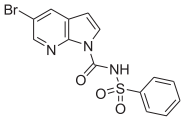	8.30 ± 0.02	2.01 ± 0.01
1g	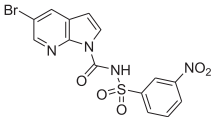	1.15 ± 0.06	2.13 ± 0.05
1h	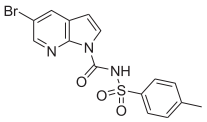	1.55 ± 0.01	0.59 ± 0.01
1i	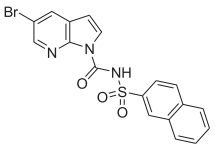	177.50 ± 4.66	25.31 ± 0.66
1j	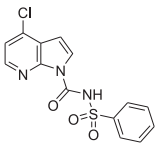	1.08 ± 0.01	26.09 ± 0.01
1k	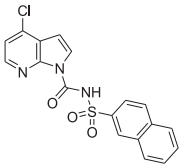	3.29 ± 0.02	1.31 ± 0.01

Table 1 (*continued*)

Compound No.	Chemical structure	IC_{50} ± S.E.M. in μM or % inhibition at 100 μM	
		NPP1	NPP3
1l	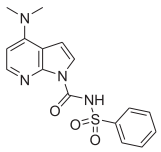	2.77 ± 0.09	0.55 ± 0.01
1m	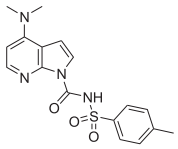	41.5%	45.7%
Suramin		7.77 ± 0.02	0.89 ± 0.16

The results are expressed as means of triplicate assays ± standard error of mean (S.E.M.).

1d) decreased the activity of both isoenzymes to a considerable level i.e., only 47.9% for NPP1 and IC_{50} = 3.72 ± 0.17 μM for NPP3. Although minor structural variation of **1d** at pyrrolopyridine core with bromine (**1h**), re-established the inhibitory potential of both isoenzymes but substitution of dimethylamino group at pyrrolopyridine scaffold (**1m**) showed limited effect on NPP1 and NPP3 activity merely by 41.5% and 45.7%, respectively. The presence of naphthalenesulfonylurea motif in compounds **1e**, **1i**, and **1k** produced interesting results. Compound **1e** with simple unsubstituted pyrrolopyridine core was devoid of inhibitory potential on both isoenzymes i.e., below 50% inhibition, whereas introduction of bromine at position 5 to pyrrolopyridine scaffold (**1i**) moderately increased the activity and this inhibitory effect was boosted up in the presence of chlorine. Comparison of SAR of structurally related compounds **1e**, **1i**, **1d** provoked that moving to substitution of more electronegative atom in the presence of naphthalenesulfonylurea moiety was much tolerated for inhibition of both NPP1 and NPP3 activity as presented in Table 1. The SAR of investigated series of compounds against NPP1 and NPP3 is summarized in Fig. 2.

2.2.1.2. Enzymes kinetics studies. Enzyme kinetic studies were carried out to interpret mode of inhibition for compounds **1c** and **1l** against NPP1 and NPP3 isozymes, respectively (Fig. 3). The plots indicate that compound **1c** inhibited the NPP1 activity in non-competitive manner whereas, the compound **1l** showed a competitive mode of inhibition for isozyme NPP3.

2.3. Effect of compounds on MCF-7 and HT-29 cancer cells viability

The cytotoxic potential of the synthesized derivatives in comparison with doxorubicin was determined by using already reported method with slight modifications [30]. Initially, the compounds were screened at 10 μM concentration against MCF-7 (breast cancer cell line) and HT-29 (colon cancer cell line). The percentage effect of compounds on cancer cells viability is shown in Table 2. The tested compounds showed minor to excellent cytotoxic potential to both cancer cell lines. The compound **1c** reduced the cells viability of MCF-7 cell lines to 70.66% whereas, the most effective compound against HT-29 was **1h** which caused the cell death of HT-29 cell lines to 82.43%. The two most cytotoxic compounds were subjected to serial dose-dependent dilutions and IC_{50} (half of maximal inhibitory concentration) values were calculated and compared with standard anticancer drug doxorubicin. The compound **1c** manifested 5.11-folds low cytotoxic effect

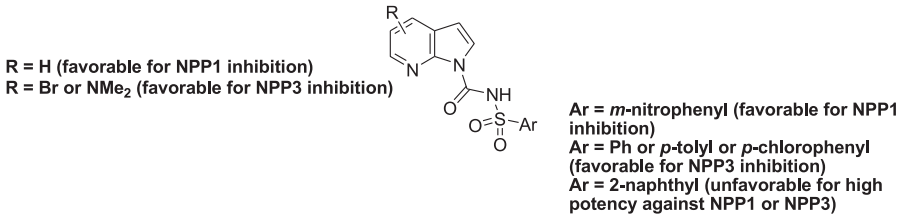

Fig. 2. A summary of SAR of the target compounds against NPP1 and NPP3.

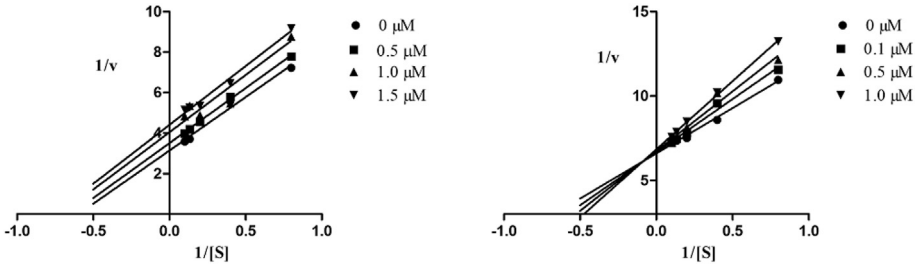

Fig. 3. Lineweaver-Burk plots of the inhibition kinetics against NPP1 by compound **1c** (left) showing uncompetitive inhibition and by compound **1l** (right) against NPP3 indicating competitive mode of inhibition.

Table 2
One-dose antiproliferative activity of the target compounds **1a-m**.

Compound No.	% inhibition of cell viability at 10 μM concentration	
	MCF-7	HT-29
1a	18.95% ± 1.80%	23.56% ± 2.36%
1b	33.45% ± 2.34%	54.36% ± 0.80%
1c	**70.66% ± 0.41%**	18.92% ± 0.34%
1d	20.30% ± 2.10%	33.40% ± 2.00%
1e	1.90% ± 0.83%	16.20% ± 0.31%
1f	16.75% ± 0.70%	14.56% ± 1.40%
1g	43.05% ± 0.38%	58.46% ± 1.20%
1h	27.96% ± 0.61%	**82.43% ± 1.29%**
1i	28.75% ± 1.51%	60.14% ± 1.90%
1j	3.32% ± 0.82%	47.57% ± 0.47%
1k	28.55% ± 0.60%	58.20% ± 0.40%
1l	26.90% ± 0.62%	17.57% ± 0.38%
1m	5.60% ± 0.50%	21.45% ± 2.56%
Doxorubicin	96.80% ± 0.70%	94.30% ± 1.10%

The results are expressed as means of triplicate assays ± S.E.M.

(IC_{50} = 4.70 ± 0.67 μM) as compared to doxorubicin (0.92 ± 0.10 μM), whereas **1h** was found with almost equally effective as doxorubicin against HT-29 cancer cell lines with an IC_{50} concentrations of 1.58 ± 0.20 μM. Most important, the compounds **1c** and **1h** showed less toxicity and higher selectivity towards normal cell lines WI-38 than doxorubicin as shown in Table 3.

Table 3
IC_{50} ± SEM values (μM) of compounds **1c**, **1h**, and doxorubicin.

Cell line	Compound No.	IC_{50} value
MCF-7	**1c**	4.70 ± 0.67 μM
	Doxorubicin	0.92 ± 0.10 μM
HT-29	**1h**	1.58 ± 0.20 μM
	Doxorubicin	1.40 ± 0.23 μM
WI-38 (normal cells)	**1c**	>20 μM
	1h	18.40 ± 1.25 μM
	Doxorubicin	1.96 ± 0.13 μM

The results are expressed as means of triplicate assays ± S.E.M.

Compound **1l** was almost equipotent to **1h** against NPP3 enzyme in cell-free assay. However, compound **1l** was much less active as antiproliferative agent against MCF-7 cell line. This can be attributed to its less hydrophobicity and ability to cross the cell membrane in whole-cell assays. Compound **1h** possessed two hydrophobic substituents (methyl and bromo) while compound **1l** lacks both groups and possesses dimethylamino group that confered more polarity.

It is noteworthy that although compounds **E** and **F** (Fig. 1) are more potent inhibitors of NPP1 and NPP3 enzymes, respectively, they exerted modest activity against MCF-7 cell line compared to compound **1c**. The inhibition percentage values of compounds **E** and **F** at 100 μM concentration against MCF-7 cell line are 40.3% and 35.6%, respectively [23].

Overexpression of NPP1 and NPP3 has been reported to be involved in propagation and metastasis of various cancers including breast, colon, lung and brain cancer cell lines. Activation of NPP1 has been found in the generation of breast cancer stem cells [31–33]. Overexpression of NPP1 was found in human brain astrocytes tumor and glioblastoma cells [13,14]. Elevated level of NPP1 was found in the HCC827, A549 lung cancer cell lines [34]. Overexpression of NPP1 and NPP3 was reported to be linked with metastasis in human colon, and bile duct carcinoma [35,36].

The exact known mechanism by which suppression of NPP1 or NPP3 leads to inhibition of metastasis and propagation of cancer cell lines is yet not known. However, there are two possibilities; one is activation and stimulation of Stimulator of Interferon Genes, also known as STING pathway and second is preservation or elevation of extracellular adenosine triphosphate (ATP) level. Activation of STING pathway leads to initiation of durable and acquired immune activity for the cure of solid tumors *in vivo* [37]. One known agonist that activates the STING receptors, present on the surface of endoplasmic reticulum is 2′, 3′ -cyclic GMP-AMP (cGAMP). cGAMP is an immunotransmitter that is regularly produced by cancerous cells and exported to the extracellular surface and level of cGAMP is regulated by hydrolase enzyme (NPP1) [38]. cGAMP contribute as a second messenger for the stimulation of STING pathway that facilitate the production of type 1 interferon and cytolytic T-cells priming. These cytokines cause the infiltration of immune cells that

facilitate to cure the cancer [37]. NPP1 hydrolyzes the cGAMP extracellularly and reduces the level of cGAMP required for the activation of STING pathway, so NPP1 is indirectly involved in propagation of cancer. Thus, inhibition or reduction of NPP1 activity by potent inhbitors might lead to cure the slighter immune associated cancers due to enhanced level of cGAMP [39]. Adenosine triphosphate plays a vital role in the suppression of transformed cancer associated fibroblasts [40], ureter cancerous cells, mast tumor cells [41], thymocytes [42], lymphocytes [43], and melanocytes [44]. ATP suppresses the propagation of human breast cancer [44], human pancreatic carcinoma, human colon cancer [45], and human prostate adenocarcinoma [46]. Moreover, hydrolysis of ATP results in elevated level of adenosine as a secondary product. Adenosine suppresses the immune response to cancer cells and facilitates cancer cells proliferation, and angiogenesis [47].

2.4. Molecular docking studies

2.4.1. Docking studies at NPP1 homology model

Docking studies of selective inhibitor of NPP1 (**1a**) revealed a wide range of interactions with amino acids residues of NPP1 homology model (Fig. 4). The binding interactions of the compounds were correlated with the already reported molecular binding study of suramin, used as standard. The complex structure of the suramin was hydrogen bonded with eight amino acid residues of NPP1 homology model that include Asn277, Ser381, Ser378, His380, Ser386, Tyr382, two H-bonds with Lys391, and two H-bond interactions with Ser387. Moreover, suramin was linked *via* amide-π stacked linkage with Ser377 and through π-π T-shaped connection with Tyr382 [48]. Compound **1a** formed hydrogen bonds with important amino acids residues including Thr256, His380 and Asn277. Moreover, **1a** was connected *via* one π-cation interaction with Gly536, one π-sulfur interaction with His424, one π-π T-shaped linkage with Lys255. Most important, compounds **1a** showed zinc metal chelation with oxygen atoms of phenyl sulfonyl and carboxamide moiety. It might be suggested that allocation of compound **1a** inside the active pocket site and important interactions such as hydrogen bonding and metal chelation contributed towards selectivity of inhibitor **1a**. Docking studies of most potent and dual inhibitor **1h** with NPP1 bindings site showed five H-bonds interactions such as Asn277 × 2, and His380 × 2 and Thr256 (Fig. 4c and d). The pyrrolo[2,3-*b*]pyridine scaffold was connected *via* three π-alkyl interactions with Lys278, similarly methyl group of *para*-methylbenzenesulfonamide ring formed two alkyl bridges with Pro453 and Phe534. Again, more importantly sulfonyl group of the **1h** showed zinc metal chelation.

2.4.2. Docking studies at NPP3 crystallographic structure

The study of putative mode of binding behavior of positive control (suramin) revealed a wide range of interactions with residues of NPP3 crystallographic structure (PDB ID = 6C01). Suramin revealed a number of hydrogen bondings with amino acids including His329, Asn290, Glu322, Leu239, Thr205, Ser326, Tyr289, Asn245, Glu275, and Glu322. Moreover, suramin was connected with Tyr289 through π-sulfur bonding; Pro288 *via* π-alkyl linkage; and zinc metal ion chelation [48]. To get insight into plausible

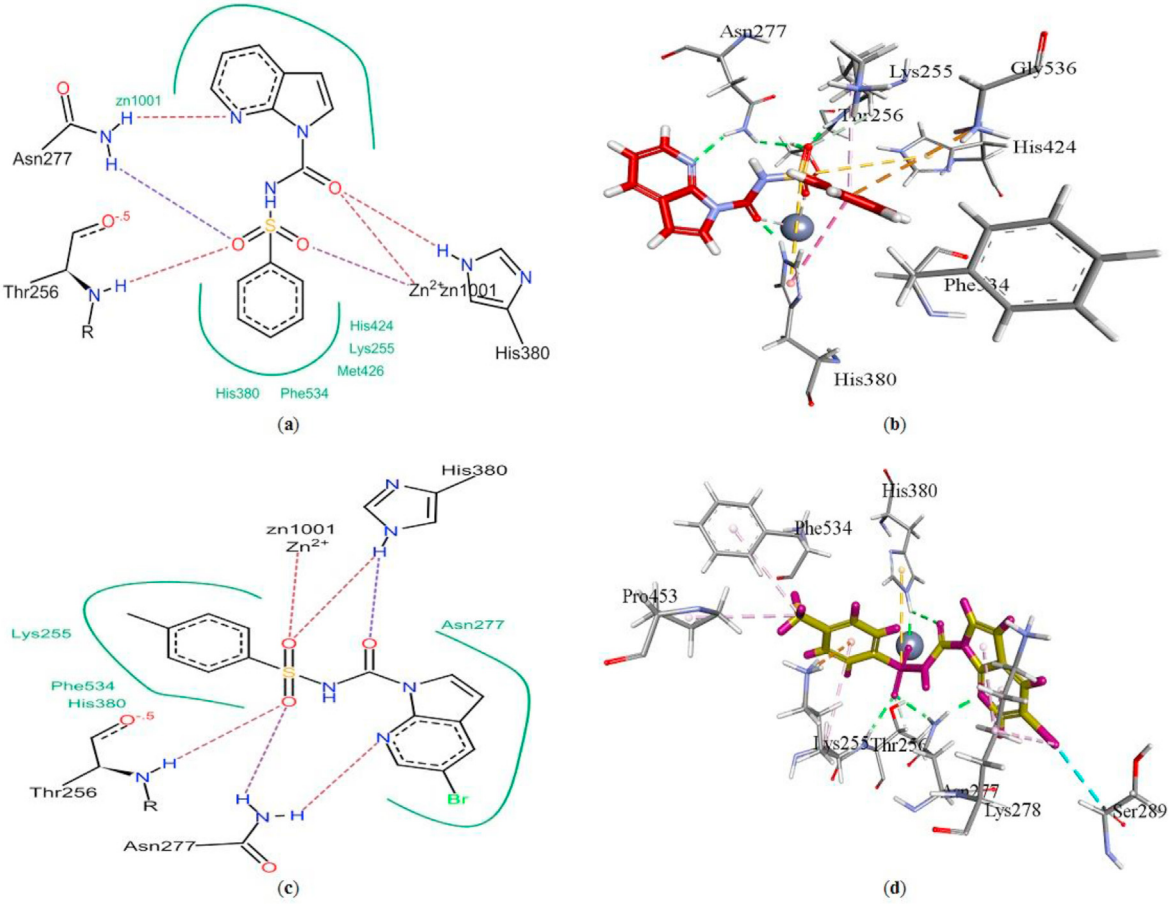

Fig. 4. 2D and 3D binding interactions and conformations of NPP1 inhibitors **1a** (Fig. 3a, b) and **1h** (Fig. 3c and d).

binding modes of interactions of selected inhibitors inside the active site of NPP3, we docked three compounds; **1b** (the most potent inhibitor), **1d** (a selective inhibitor), and **1h** (a dual inhibitor) as shown in Fig. 5. The carboxamide and sulfonyl groups of compound **1b** were connected *via* hydrogen bonds with Asn226, Thr205, and His483 (Fig. 5a - b). The pyrrolo[2,3-*b*]pyridine scaffold showed two π-π stacked linkages with His329 and also *para*-chlorophenyl moiety was connected through π and π-alkyl interaction with Leu239. Again, oxygen atom of sulfonyl group was chelated with zinc-metal ion, contributing to the potency and selectivity of compound **1b**. The docking studies of selective inhibitor of NPP3 (**1d**) demonstrated almost same binding interactions as the most potent inhibitor **1b**. The selectivity of **1d** vs **1b** might be attributed to the presence of tolyl ring instead of chlorophenyl ring in **1b**. The binary inhibitor **1h** showed a wide range of interactions with residues of pocket site. Compound **1h** was stabilized through H-bonds with Asn226, Lys204, and His483. In addition, **1h** was surrounded by His329, Thr205, Phe206, and Leu239. Most important, both rings of the pyrrolo[2,3-*b*]pyridine core were chelated with zinc cation.

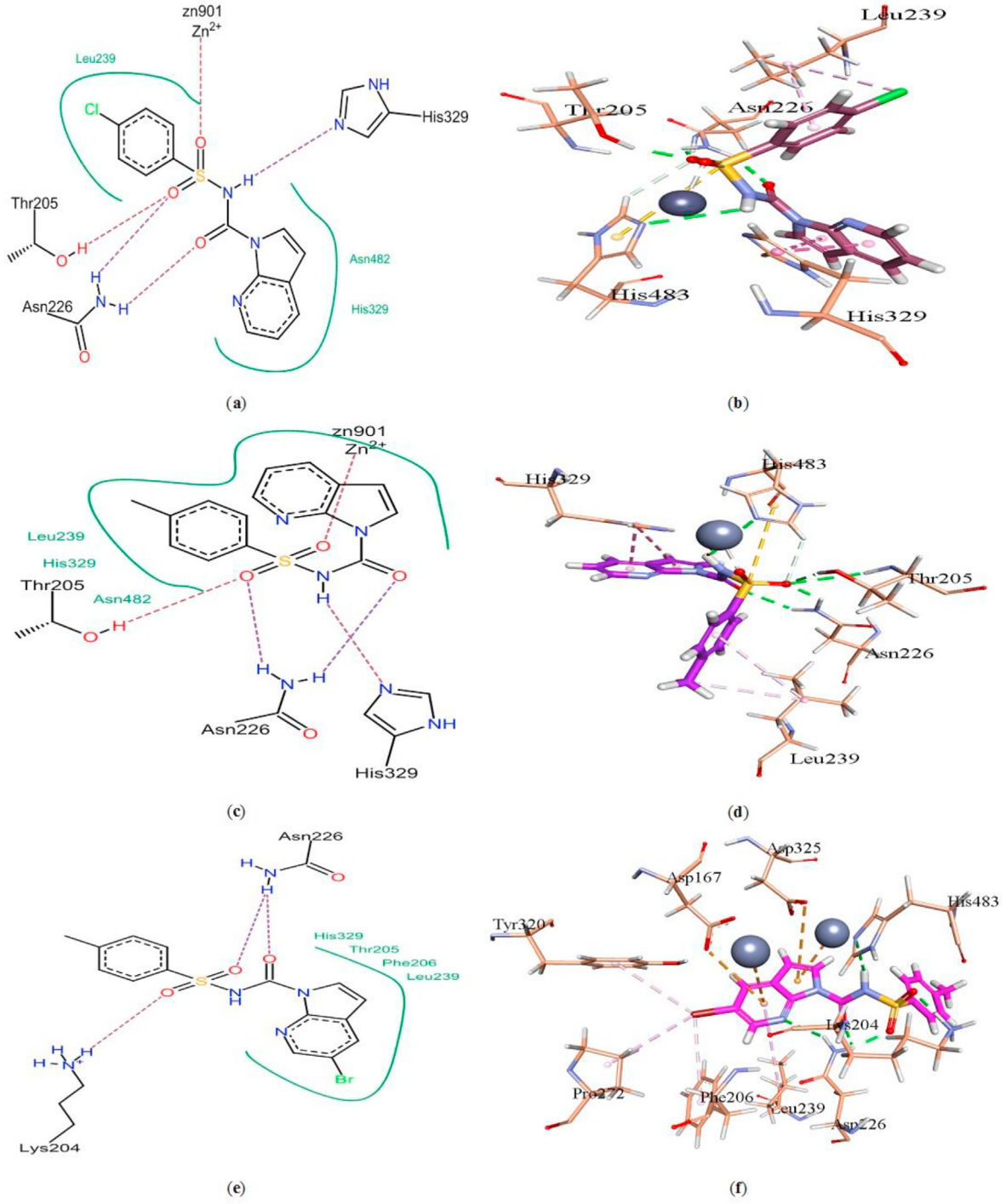

Fig. 5. 2D and 3D binding interactions and conformations of NPP3 inhibitors; **1b** (Fig. 5a, b), **1d** (Fig. 5c, d), and **1h** (Fig. 5e and f).

2.5. In vivo effect of compound **1h** on blood glucose level in mice

Sulfonylurea derivatives are known as hypoglycemic agents [49,50]. Due to the presence of sulfonylurea moiety in the target compound structures, we decided to investigate the effect of compound **1h**, the most potent antiproliferative compound, on blood glucose level in mice. The compound was injected intraperitoneally to male BALB/c mice at a dose of 10 or 20 mg/kg body weight. The blood glucose level was measured for each mouse at 30-min time intervals over 2 h, and the results are illustrated in Table 4. It is obvious that compound **1h** did not produce significant hypoglycemic effect, which is an important merit.

3. Conclusion

The target sulfonylurea-bearing pyrrolo[2,3-*b*]pyridine derivatives were synthesized and evaluated for their potential to inhibit NPP1 and NPP3 enzymatic activity. The calculated inhibitory effect was compared with the reference standard inhibitor, suramin. We discovered selective, dual, and even more active inhibitors of both NPP1 and NPP3 than suramin (standard drug). Compound **1a** was identified as selective inhibitor of NPP1 with an IC_{50} value of 4.50 ± 0.16 μM, whereas compound **1d** was found as selective inhibitor of NPP3 with an IC_{50} value of 3.72 ± 0.17 μM. Similarly, compound **1c** was identified as the most potent inhibitor of NPP1 (0.80 ± 0.04 μM), and **1l** had strongest inhibitory activity on NPP3 (IC_{50} = 0.55 ± 0.01 μM). The kinetic studies showed that compound **1c** was an uncompetitive inhibitor of isoenzyme NPP1 and the compound **1l** was a competitive inhibitor of isozyme NPP3. Molecular docking studies of the strongest inhibitors either for NPP1 (**1a** and **1h**) or NPP3 (**1b**, **1d**, and **1h**) showed promising binding interactions with active site residues of both isozymes, where the sulfonamide group formed zinc metal ion chelation. Also, cytotoxic examination of these compounds against MCF-7 and HT-29 cancer cell lines revealed **1c** as most chemoselective against MCF-7 cell lines with an IC_{50} value of 4.70 ± 0.67 μM, and **1h** proved as the most cytotoxic agent against HT-29 cancer cell line with an IC_{50} value of 1.58 ± 0.20 μM. The IC_{50} values revealed that compounds **1c** and **1h** were more selective and less toxic to WI-38 normal cell line as compared to standard doxorubicin for MCF-7 and HT-29 cancer cell lines, respectively. This study led to discovery of a new sulfonylurea-based antiproliferative agent **1h** that does not produce hypoglycemia as a side effect. It is almost equipotent to doxorubicin against HT-29 colon cancer cell line with the merit of higher selectivity index towards cancer cells than normal cells than doxorubicin. Its molecular mechanism of action could be, at least in part, inhibition of NPP1 and NPP3 isozymes. Considering the high potency of compounds **E** and **F** (Fig. 1) against NPP1 and NPP3, respectively, we recommend investigating the impact of sulfonamide or thiourea spacers on activity in the future.

Table 4
Mean blood glucose levels (mg/dL) in mice after i.p. injection of compound **1h** at doses of 10 or 20 mg/kg.

Time after injection (min)	Control	10 mg/kg	20 mg/kg
0	124 ± 9	108 ± 5	114 ± 7
30	106 ± 5	103 ± 7	113 ± 8
60	141 ± 6	122 ± 2	114 ± 14
90	115 ± 7	124 ± 12	128 ± 6
120	120 ± 4	121 ± 9	121 ± 7

The results are expressed as means ± standard deviation (S.D.), $n = 5$ in all groups.

4. Experimental

4.1. General

The melting points were measured on a Stuart melting point apparatus (Staffordshire, UK), and are uncorrected. Bruker Avance (400 MHz spectrometer) was used to analyze the compounds by ^1H and ^{13}C NMR. LC-MS analysis was carried out by LC-MS analyzer (Waters Corporation, MA, USA). All the solvents and reagents were purchased from commercial companies and used as such. The final and intermediate compounds were purified by flash column chromatography (silica gel, pore size 0.040–0.063 mm, 230–400 mesh) using laboratory reagent grade solvents.

4.2. Chemical synthesis of compounds

4.2.1. Synthesis of the aryl sulfonamide reagents ***4a-e***

To a solution of arylsulfonyl chloride **2a-e** (0.1 mmol) in methanol (5 mL), ammonium hydroxide (33% solution, 5 mL) was added. The reaction mixture was stirred at room temperature for 5–10. Reaction completion was confirmed by TLC then LC-MS. After that, the reaction mixture was evaporated under reduced pressure to dryness. Water (10 mL) and ethyl acetate (10 mL) were added to the residue for extraction. The ethyl acetate layer was separated, washed with saturated saline (3 × 5 mL), dried using anhydrous Na_2SO_4, and evaporated to dryness to obtain the title compounds as solid products. They were used in the next step as such.

4.2.2. Synthesis of 4-(dimethylamino)-7-azaindole (**7**)

A mixture of compound **5c** (152 mg, 1 mmol) was fused with dimethylammonium chloride (405 mg, 5 mmol) in oil bath without solvent at 180 °C for 5 h. The reaction mixture was cooled, extracted with ethyl acetate (20 mL), and washed with saline (20 mL). The organic layer was separated, dried using anhydrous Na_2SO_4, filtered, and evaporated to dryness. The product was purified by column chromatography (silica gel, dichloromethane:methanol 10:1 v/v) to obtain the title product (yield: 30%, R_f = 0.54 dichloromethane:methanol 10:1 v/v).

^1H NMR ($CDCl_3$, 400 MHz) δ 11.20 (brs, 1H), 7.92 (d, J = 5.6 Hz, 1H), 7.04 (d, J = 3.6 Hz, 1H), 6.51 (d, J = 3.6 Hz, 1H), 6.06 (d, J = 5.6 Hz, 1H), 3.11 (s, 6H).

4.2.3. Synthesis of carbamate intermediates ***9a-d***

A mixture of compound **5a-c** or **7** (1 mmol) and TEA (2 mL) in anhydrous THF (5 mL) was cooled to 0 °C using ice bath. A solution of phenyl chloroformate (222 mg, 2 mmol) in anhydrous THF (5 mL) was added slowly thereto. The mixture was further stirred at the same temperature for 2 h. The reaction mixture was evaporated in vacuo, extracted with ethyl acetate (20 mL), and washed with saline (20 mL). The organic layer was separated, dried using anhydrous Na_2SO_4, filtered, and evaporated to dryness. It was used in the next reaction with no further purification.

4.2.4. Synthesis of the target sulfonyl urea products ***1a-m***

A mixture of compound **9a-d** (0.1 mmol), **4a-e** (0.12 mmol), and anhydrous potassium carbonate (69 mg, 0.5 mmol) in dry dichloromethane (5 mL) was allowed to stir at room temperature overnight. After reaction completion, the mixture was washed with water (5 mL) and the organic layer was separated, dried with anhydrous Na_2SO_4, filtered, and evaporated to dryness. The remaining residue was purified by column chromatography.

*4.2.4.1. N-(Pyrrolo[2,3-b]pyridine-1-carbonyl)benzenesulfonamide (**1a**).* Purification was carried out by flash column chromatography (silica gel, hexane:ethyl acetate 3:1 v/v then switching to ethyl

acetate); yield: 51%; mp: 130–132 °C; ^{1}H NMR ($CDCl_3$, 400 MHz) δ 8.33 (brs, 1H), 7.88 (d, J = 8.0 Hz, 2H), 7.72–7.67 (m, 1H), 7.55–7.43 (m, 2H), 7.19 (d, J = 7.6 Hz, 1H), 7.04–7.00 (m, 2H), 6.90–6.82 (m, 2H); ^{13}C NMR ($CDCl_3$, 100 MHz) δ 155.8, 142.0, 132.7, 129.6, 129.1, 128.3, 127.8, 126.4, 125.5, 121.9, 115.4; LC/MS *m/z*: 302.0 (M^+ + 1); CHN analysis: calculated C:55.80%, H:3.68%, N:13.95%; found: C:55.70%, H:3.74%, N:13.89%.

*4.2.4.2. N-(Pyrrolo[2,3-b]pyridine-1-carbonyl)-4-chlorobenzenesulfonamide (**1b**).* Purification was carried out by flash column chromatography (silica gel, hexane:ethyl acetate 3:1 v/v then switching to ethyl acetate); yield: 52%; mp: >280 °C; ^{1}H NMR (DMSO-d_6, 400 MHz) δ 8.29 (d, J = 8.5 Hz, 1H), 7.95–7.89 (m, 5H), 7.50 (d, J = 8.5 Hz, 2H), 7.14–7.12 (m, 1H), 6.46–6.44 (m, 1H); ^{13}C NMR ($CDCl_3$, 100 MHz) δ 155.9, 140.6, 137.7, 132.8, 130.1, 128.2, 127.2, 124.2, 118.9, 117.9, 104.8, 103.6; LC/MS *m/z*: 336.0 (M^+ + 1); CHN analysis: calculated C:50.08%, H:3.00%, N:12.51%; found: C:50.34%, H:2.89%, N:12.45%.

*4.2.4.3. N-(Pyrrolo[2,3-b]pyridine-1-carbonyl)-3-nitrobenzenesulfonamide (**1c**).* Purification was carried out by flash column chromatography (silica gel, hexane:ethyl acetate 3:1 v/v then switching to ethyl acetate); yield: 45%; mp: 171–172 °C; ^{1}H NMR (CD_3OD, 400 MHz) δ 8.61 (brs, 2H), 8.36–8.34 (m, 2H), 8.18–8.16 (m, 2H), 7.74–7.70 (m, 3H); ^{13}C NMR (CD_3OD, 100 MHz) δ 155.9, 146.2, 143.2, 140.7, 139.4, 139.4, 132.6, 130.1, 128.7, 126.5, 123.9, 118.9, 118.0, 103.9; LC/MS *m/z*: 347.0 (M^+ + 1); CHN analysis: calculated C:48.55%, H:2.91%, N:16.18%; found: C:48.64%, H:2.83%, N:16.15%.

*4.2.4.4. N-(Pyrrolo[2,3-b]pyridine-1-carbonyl)-4-methylbenzenesulfonamide (**1d**).* Purification was carried out by flash column chromatography (silica gel, hexane:ethyl acetate 3:1 v/v then switching to ethyl acetate); yield: 75%; mp: 150–151 °C; ^{1}H NMR ($CDCl_3$, 400 MHz) δ 8.28 (brs, 1H), 8.19–7.91 (m, 2H), 7.87–7.68 (m, 2H), 7.53 (d, J = 8.0 Hz, 1H), 7.09 (d, J = 8.0 Hz, 1H), 6.81 (d, J = 5.2 Hz, 1H), 6.78–6.50 (m, 1H), 6.23 (brs, 1H), 2.25 (s, 3H, Me); ^{13}C NMR (DMSO-d_6, 100 MHz) δ 143.2, 142.5, 142.0, 141.4, 129.4, 128.4, 128.1, 127.3, 126.0, 125.7, 115.5, 99.8, 21.0; LC/MS *m/z*: 316.0 (M^+ + 1); CHN analysis: calculated C:57.13%, H:4.16%, N:13.33%; found: C:57.02%, H:4.08%, N:13.43%.

*4.2.4.5. N-(Pyrrolo[2,3-b]pyridine-1-carbonyl)-2-naphthalenesulfonamide (**1e**).* Purification was carried out by flash column chromatography (silica gel, hexane:ethyl acetate 3:1 v/v then switching to hexane:ethyl acetate 1:1 v/v); yield: 36%; mp: 229–231 °C (dec.); ^{1}H NMR (CD_3OD, 400 MHz) δ 8.40 (brs, 1H), 8.34 (s, 1H), 8.03–7.89 (m, 4H), 7.85–7.79 (m, 2H), 7.75–7.69 (m, 2H), 7.55–7.48 (m, 2H), 7.42–7.37 (m, 1H); ^{13}C NMR (CD_3OD, 100 MHz) δ 143.1, 140.6, 134.6, 132.2, 129.6, 128.8, 128.7, 128.2, 128.0, 127.6, 127.4, 127.1, 126.6, 126.2, 122.9, 121.7, 102.5; LC/MS *m/z*: 352.0 (M^+ + 1); CHN analysis: calculated C:61.53%, H:3.73%, N:11.96%; found: C:61.45%, H:3.58%, N:12.06%.

*4.2.4.6. N-(5-Bromopyrrolo[2,3-b]pyridine-1-carbonyl)benzenesulfonamide (**1f**).* Purification was carried out by flash column chromatography (silica gel, hexane:ethyl acetate 4:1 v/v then switching to hexane:ethyl acetate 1:1 v/v); yield: 44%; mp: 141–143 °C; ^{1}H NMR ($CDCl_3$, 400 MHz) δ 7.80–7.70 (m, 4H), 7.55 (d, J = 8.0 Hz, 1H), 7.44 (t, J = 7.2 Hz, 1H), 7.19–7.10 (m, 2H), 6.95–6.73 (m, 2H); ^{13}C NMR ($CDCl_3$, 100 MHz) δ 145.2, 132.6, 132.5, 131.8, 131.7, 129.5, 129.0, 128.4, 126.3, 115.4, 112.5, 102.2; LC/MS *m/z*: 380.9 (M^+ + 2), 379.9 (M^+ + 1); CHN analysis: calculated C:44.22%, H:2.65%, N:11.05%; found: C:44.40%, H:2.55%, N:10.97%.

*4.2.4.7. N-(5-Bromopyrrolo[2,3-b]pyridine-1-carbonyl)-3-nitrobenzenesulfonamide (**1g**).* Purification was carried out by flash column chromatography (silica gel, hexane:ethyl acetate 2:1 v/v then switching to ethyl acetate); yield: 75%; mp: 227–230 °C; ^{1}H NMR ($CDCl_3$, 400 MHz) δ 8.59–8.28 (m, 2H), 8.15–7.93 (m, 3H), 7.71 (brs, 1H), 7.47–7.35 (m, 1H), 6.94 (d, J = 12.8 Hz, 1H), 6.76–6.72 (m, 1H); ^{13}C NMR ($CDCl_3$, 100 MHz) δ 145.3, 132.8, 132.6, 131.9, 131.7, 129.6, 129.1, 128.6, 126.5, 115.5, 112.7, 102.3; LC/MS *m/z*: 425.9 (M^+ + 2), 424.9 (M^+ + 1); CHN analysis: calculated C:39.54%, H:2.13%, N:13.18%; found: C:39.40%, H:2.08%, N:13.30%.

*4.2.4.8. N-(5-Bromopyrrolo[2,3-b]pyridine-1-carbonyl)-4-methylbenzenesulfonamide (**1h**).* Purification was carried out by flash column chromatography (silica gel, hexane:ethyl acetate 4:1 v/v then switching to hexane:ethyl acetate 1:1 v/v); yield: 78%; mp: 130–132 °C; ^{1}H NMR ($CDCl_3$, 400 MHz) δ 12.54 (brs, 1H), 8.43 (s, 1H), 8.08 (t, J = 7.6 Hz, 2H), 7.91 (d, J = 7.2 Hz, 1H), 7.82 (s, 1H), 7.37–7.29 (m, 2H), 6.56 (s, 1H), 2.44 (s, 3H); ^{13}C NMR (DMSO-d_6, 100 MHz) δ 143.2, 142.4, 141.9, 141.4, 130.1, 129.7, 129.4, 129.1, 128.1, 127.7, 127.5, 125.7, 99.7, 21.0; LC/MS *m/z*: 395.0 (M^+ + 2), 394.0 (M^+ + 1); CHN analysis: calculated C:45.70%, H:3.07%, N:10.66%; found: C:45.52%, H:3.02%, N:10.74%.

*4.2.4.9. N-(5-Bromopyrrolo[2,3-b]pyridine-1-carbonyl)-2-naphthalenesulfonamide (**1i**).* Purification was carried out by flash column chromatography (silica gel, hexane:ethyl acetate 5:1 v/v then switching to hexane:ethyl acetate 2:1 v/v); yield: 30%; mp: 222–224 °C; ^{1}H NMR ($CDCl_3$, 400 MHz) δ 8.51 (d, J = 6.4 Hz, 1H), 7.95–7.93 (m, 4H), 7.70–7.56 (m, 4H), 7.43–7.29 (m, 3H); ^{13}C NMR ($CDCl_3$, 100 MHz) δ 143.3, 140.7, 134.8, 132.4, 129.7, 129.0, 128.8, 128.4, 128.1, 127.8, 127.5, 127.3, 126.7, 126.4, 123.1, 121.8, 102.7; LC/MS *m/z*: 431.0 (M^+ + 2), 430.0 (M^+ + 1); CHN analysis: calculated C:50.25%, H:2.81%, N:9.77%; found: C:50.13%, H:2.98%, N:9.66%.

*4.2.4.10. N-(4-Chloropyrrolo[2,3-b]pyridine-1-carbonyl)benzenesulfonamide (**1j**).* Purification was carried out by flash column chromatography (silica gel, hexane:ethyl acetate 3:1 v/v then switching to ethyl acetate); yield: 68%; mp: 225–228 °C (dec.); ^{1}H NMR ($CDCl_3$, 400 MHz) δ 8.40–8.21 (m, 1H), 7.94–7.85 (m, 2H), 7.66–7.46 (m, 3H), 6.92 (s, 2H), 6.73 (d, J = 4.0 Hz, 1H), 6.65–6.57 (m, 1H); ^{13}C NMR ($CDCl_3$, 100 MHz) δ 145.1, 132.5, 132.3, 131.7, 131.5, 129.4, 128.9, 128.2, 126.2, 115.3, 112.4, 102.3; LC/MS *m/z*: 337.0 (M^+ + 2), 336.0 (M^+ + 1); CHN analysis: calculated C:50.08%, H:3.00%, N:12.51%; found: C:49.96%, H:2.88%, N:12.60%.

*4.2.4.11. N-(4-Chloropyrrolo[2,3-b]pyridine-1-carbonyl)-2-naphthalenesulfonamide (**1k**).* Purification was carried out by flash column chromatography (silica gel, hexane:ethyl acetate 2:1 v/v then switching to ethyl acetate); yield: 56%; mp: 152–153 °C; ^{1}H NMR ($CDCl_3$, 400 MHz) δ 8.53 (brs, 1H), 7.97–7.87 (m, 4H), 7.67–7.59 (m, 4H), 7.52–7.43 (m, 3H); ^{13}C NMR ($CDCl_3$, 100 MHz) δ 143.4, 140.8, 134.9, 132.6, 129.8, 129.2, 128.9, 128.6, 128.2, 128.0, 127.6, 127.5, 126.9, 126.5, 123.2, 121.9, 102.9; LC/MS *m/z*: 387.0 (M^+ + 2), 386.0 (M^+ + 1); CHN analysis: calculated C:56.03%, H:3.13%, N:10.89%; found: C:56.09%, H:3.05%, N:10.96%.

*4.2.4.12. N-[4-(Dimethylamino)pyrrolo[2,3-b]pyridine-1-carbonyl]benzenesulfonamide (**1l**).* Purification was carried out by flash column chromatography (silica gel, ethyl acetate then switching to ethyl acetate:methanol 5:1 v/v); yield: 50%; mp: >280 °C; ^{1}H NMR ($CDCl_3$, 400 MHz) δ 8.13–7.88 (m, 3H), 7.68 (d, J = 8.0 Hz, 2H), 7.46 (brs, 3H), 6.88–6.66 (m, 2H), 3.41 (s, 6H); ^{13}C NMR ($CDCl_3$, 100 MHz) δ 156.7, 153.5, 147.5, 142.0, 137.7, 137.0, 129.0, 128.4, 127.3, 105.3, 101.9, 100.7, 41.9; LC/MS *m/z*: 345.1 (M^+ + 1); CHN analysis: calculated C:55.80%, H:4.68%, N:16.27%; found: C:55.85%, H:4.80%, N:16.15%.

*4.2.4.13. N-[4-(Dimethylamino)pyrrolo[2,3-b]pyridine-1-carbonyl]-4-methylbenzenesulfonamide (**1m**).* Purification was carried out by flash column chromatography (silica gel, ethyl acetate then switching to ethyl acetate:methanol 6:1 v/v); yield: 68%; mp: 220–223 °C (dec.); ^{1}H NMR ($CDCl_3$, 400 MHz) δ 8.02–7.99 (m, 3H), 7.64 (d, J = 8.0 Hz, 2H), 7.21 (brs, 1H), 6.75 (d, J = 8.0 Hz, 1H), 6.69 (d, J = 4.0 Hz, 1H), 6.41 (d, J = 6.4 Hz, 1H), 3.73 (s, 6H), 2.34 (s, 3H); ^{13}C NMR ($CDCl_3$, 100 MHz) δ 156.6, 153.4, 147.3, 141.9, 137.6, 136.8, 128.9, 128.3, 127.1, 105.2, 101.8, 100.6, 41.8, 21.7; LC/MS *m/z*: 359.1 (M^+ + 1); CHN analysis: calculated C:56.97%, H:5.06%, N:15.63%; found: C:56.80%, H:4.98%, N:15.74%.

4.3. Enzyme testing

4.3.1. Transfection of COS-7 cells

COS-7 cells were transfected by using human NPP1 and NPP3 expressing plasmids. For this purpose, 10 cm plates were used and the Dulbecco's Modified Eagle Medium/F-12 (DMEM/F-12) was used for the incubation of confluent cells with plasmid DNA (6 μg) and Lipofectamine (without fetal bovine serum). The process of transfection was stopped by adding an equal volume of DMEM/F-12 (with 20% FBS). The transfected cells were harvested 48–72 h later [51].

4.3.2. Collection of membrane fractions

The harvested transfected cells were subjected to washing by using Tris-saline buffer at 4 °C. The scraping and collection of the cells were carried out in harvesting buffer (95 mM NaCl, 0.1 mM phenylmethylsulfonyl fluoride, and 45 mM Tris) at pH 7.5. The cells were centrifuged twice 5 min each at 300 g and 4 °C. After that, the cells were resuspended in harvesting buffer with aprotinin 10 mg/mL and subjected to sonication. Again, cells were centrifuged at 300 g for 10 min and cellular debris was discarded. In the supernatant, 7.5% glycerol was added and preserved at −80 °C. The Bradford microplate assay was used for the estimation of protein contents, using Bovine serum albumin as a standard [52].

4.3.3. NPP1 and NPP3 isoenzymes inhibition assay

The inhibitory effect of compounds **1a-m** was determined by using already reported method with slight modifications [53]. The assay buffer was composed of Tris. HCl (50 mM), $MgCl_2$ (5 mM) and $ZnCl_2$ (0.1 mM) with final pH 9.5. The assay was performed in 96-well plate with each well containing assay buffer, 100 μM of test compound, enzymes NPP1 (27 ng), NPP3 (35 ng) and substrate *p*-nitrophenyl 5′-thymidine monophosphate. The plate was placed for 35 min in an incubator and read was taken at the wavelength of 405 nm by using microplate reader (BioTek FLx800, Instruments, Inc. USA). The compounds showing more than 50% inhibition of either of isozyme (NPP1 or NPP3) were subjected to serial dilutions for the determination of IC_{50} values. The data was analyzed by using non-linear regression analysis curve fitting program PRISM 5.0 (Graph Pad, San Diego, California, USA).

4.3.4. Enzyme kinetics studies

For the determination of kinetic studies, the used substrate concentration were 0.0 mM, 1.25 mM, 2.50 mM, 5.0 mM, 7.5 mM, and 10.0 mM. The final assay concentrations for the compound **1c** were 0.0 μM, 0.5 μM, 1.0 μM, 1.5 μM and similarly for the compound **1l**, we used the assay concentrations 0.0 μM, 0.1 μM, 0.5 μM, 1.0 μM. The substrate and the compounds (**1c**, **1l**) were incubated with assay buffer that was comprised of Tris. HCl (50 mM), $MgCl_2$ (5 mM) and $ZnCl_2$ (0.1 mM) with final pH 9.5. The reaction mixture was incubated at 37 °C, and the reading was taken for 35 min with 05 min intervals. The microplate reader (BioTek FLx800, Instruments Inc., USA) was used for reading at 405 nm. Lineweaver-Burk plots for the both compounds were plotted with the help of linear regression analysis of PRISM 5.0 (Graph Pad, San Diego, California, USA).

4.4. Antiproliferative activity

4.4.1. Cell culture

The breast cancer cell line (MCF-7), and colorectal adenocarcinoma cell line (HT-29) were collected from the European Collection of Cell Cultures (ECACC, UK) and later on, maintained in Roswell Park Memorial Institute medium (RPMI, Sigma-Aldrich, St. Louis, MO, USA). The normal diploid human fibroblasts (WI-38), were kindly gifted by Prof. Ekkehard Dikomey (University Cancer Center, Hamburg University, Hamburg, Germany), that were preserved by using Dulbecco's Modified Eagle Medium (DMEM, Sigma-Aldrich) supplemented with 10% concentration of fetal bovine serum and antibiotics 1% of penicillin/streptomycin, obtained from Sigma-Aldrich.

4.4.2. MTT assay

The 3-(4,5-dimethylthiazol-2-yl)-2,5-diphenyltetrazolium bromide assay (MTT) was carried out to examine the chemotherapeutic effect of the tested compounds on cancer cells viability. The assay was performed according to already reported method with few modifications [54]. The tested compounds were dissolved in DMSO to prepare 10 mM stock solution then diluted by dissolution in fetal bovine serum which is used as an incubation medium. The experimental cell lines were seeded at a density of 4×10^4 per well in tissue culturing plate and placed for overnight incubation. The incubated plates were treated with target compounds, positive control (doxorubicin), and negative control dimethyl sulfoxide 24 h. After 24 h, the cell media was separated and again cells were treated with approximately 200 mL of media with MTT tetrazolium dye (0.5 mg/mL) and incubated at 37 °C for 2 h. Again, media were removed and the violet crystals were solubilized by adding 200 mL of DMSO. Finally, the microplate reader (Thermo Scientific, Massachusetts, USA) was used for the measurement of wavelength at 570 nm.

4.5. Molecular docking studies

For the purpose of molecular docking studies, a previously generated homology model of NPP1 (PDB ID 4GTW) was used [55]. However, for NPP3, a crystallographic structure with PDB ID 6C01 was downloaded from Protein Data Bank [56]. For the preparation of database of selected inhibitors and energy minimization, Molecular Operating Environment (MOE 2014–0901) was used [57]. Structures of both proteins NPP1 and NPP3 were prepared and docked by using LeadIT (BioSolveIT GmbH, Germany) [58]. The poses possessing high affinity and low binding energy were selected for visualization by using Discovery Studio Visualizer DS [59].

4.6. In vivo effect of blood glucose level in mice

The protocol was approved by Research Ethics Committee at Dubai Pharmacy College for Girls, Dubai, United Arab Emirates (Reference #REC/FD/2020/03). Compound **1h** was dissolved in a solution of (2-hydroxypropyl)-β-cyclodextrin in distilled water (40% w/v) to make a 1 mg/mL solution. The resultant solution was injected i.p. to male BALB/c mice (30–35 g body weight) in a dose of 10 or 20 mg/kg. A control group was injected with placebo, (2-hydroxypropyl)-β-cyclodextrin solution devoid of compound **1h**. The number of mice is five per group. The blood glucose level was measured at 0, 30, 60, 90, and 120 min intervals for each animal as

per the kit's instructions. The mice were deprived from any access to diet during the 2-h measurement period following the injection.

Declaration of competing interest

None.

Acknowledgment

This work was funded by University of Sharjah, Dubai Pharmacy College for Girls, United Arab Emirates as well as by the German Academic Exchange Service (DAAD) "German-Pakistani Research Collaboration Programme". J.S. received support from the Natural Sciences and Engineering Research Council of Canada (NSERC; RGPIN-2016-05867).

References

[1] F. Kukulski, S.A. Levesque, J. Sevigny, Impact of ectoenzymes on p2 and p1 receptor signaling, Adv. Pharmacol. 61 (2011) 263–299.
[2] S.C. Robson, J. Sévigny, H. Zimmermann, The E-NTPDase family of ectonucleotidases: structure function relationships and pathophysiological significance, Purinergic Signal. 2.2 (2006) 409.
[3] J. Iqbal, S.A. Levesque, J. Sévigny, C.E. Mueller, A highly sensitive CE-UV method with dynamic coating of silica-fused capillaries for monitoring of nucleotide pyrophosphatase/phosphodiesterase reactions, Electrophoresis 29 (2008) 3685–3693, 17.
[4] H. Zimmermann, M. Zebisch, N. Sträter, Cellular function and molecular structure of ecto-nucleotidases, Purinergic Signal.. 8.3 (1012) 437-502.
[5] J.W. Goding, B. Grobben, H. Slegers, Physiological and pathophysiological functions of the ecto-nucleotide pyrophosphatase/phosphodiesterase family, Biochim. Biophys. Acta (BBA) - Mol. Basis Dis. 1638 (2003) 1–19.
[6] R. Terkeltaub, Physiologic and pathologic functions of the NPP nucleotide pyrophosphatase/phosphodiesterase family focusing on NPP1 in calcification, Purinergic Signal. 2 (2) (2006) 371–377.
[7] F. Rutsch, S. Vaingankar, K. Johnson, I. Goldfine, B. Maddux, P. Schauerte, H. Kalhoff, K. Sano, W.A. Boisvert, A. Superti-Furga, R. Terkeltaub, PC-1 nucleoside triphosphate pyrophosphohydrolase deficiency in idiopathic infantile arterial calcification, Am. J. Pathol. 158 (2001) 543–554.
[8] N. Ruf, B. Uhlenberg, R. Terkeltaub, P. Nurnberg, F. Rutsch, The mutational spectrum of NPP1 as arising after the analysis of 23 unrelated patients with generalized arterial calcification of infancy (GACI), Hum. Mutat. 26 (2005) 98.
[9] L. Chang, S.Y. Lee, P. Leonczak, J. Rozenski, S. De Jonghe, T. Hanck, C.E. Muller, P. Herdewijn, Imidazopyridine-and purine-thioacetamide derivatives: potent inhibitors of nucleotide pyrophosphatase/phosphodiesterase 1 (NPP1), J. Med. Chem. 57 (2014) 10080–10100.
[10] A. Mahmut, M.C. Boulanger, R. Bouchareb, F. Hadji, P. Mathieu, Adenosine derived from ecto-nucleotidases in calcific aortic valve disease promotes mineralization through A2a adenosine receptor, Cardiovascular, Res. 106 (2015) 109–120.
[11] I.D. Goldfine, B.A. Maddux, J.F. Youngren, G. Reaven, D. Accili, V. Trischitta, R. Vigneri, L. Frittitta, The role of membrane glycoprotein plasma cell antigen 1/ectonucleotide pyrophosphatase phosphodiesterase 1 in the pathogenesis of insulin resistance and related abnormalities, Endocr. Rev. 29 (2008) 62–75.
[12] B. Grobben, P.P. De Deyn, H. Slegers, Rat C6 glioma as experimental model system for the study of glioblastoma growth and invasion, Cell Tissue Res. 310 (2002) 257–270.
[13] I. Aerts, J.J. Martin, P.P. De Deyn, C. Van Ginniken, X. Van Ostade, M. Kockx, G. Dua, H. Slegers, The expression of ecto-nucleotide pyrophosphatase/phosphodiesterase 1 (E-NPP1) is correlated with astrocytic tumor grade, Clin. Neurol. Neurosurg. 113 (2011) 224–229.
[14] J. Bageritz, L. Puccio, P. Rm, V. Hovestadt, E. Phillips, T. Pankert, J. Lohr, P. Lichter, V. Goidts, Stem cell characteristics in glioblastoma are maintained by the ectonucleotidases E-NPP1, Cell Death Differ. 21 (2014) 929–940.
[15] C. Stefan, S. Jansen, M. Bollen, Modulation of purinergic signaling by NPP-type ectophosphodiesterases, Purinergic Signal. 2 (2006) 361–370.
[16] H.J. Buhring, A. Streble, P. Valent, The basophilspecific ectoenzyme E-NPP3 (CD203c) as a marker for cell activation and allergy diagnosis, Int. Arch. Allergy Immunol. 133 (2004) 317–329.
[17] A. Buffon, E.A. Casali, V.V. Cardoso, L.F. Zerbini, S.C. Robson, J.J.F. Sarkis, M.R. Wink, Differential expression of nucleotide pyrophosphatase/phosphodiesterases by Walker 256 mammary cancer cells in solid tumors and malignant ascites, Life Sci. 86 (2010) 435.
[18] R.J. Fox, N.L. Cuniere, L. Bakrania, C. Wei, N.A. Strotman, M. Hay, D. Fanfair, C. Regens, G.L. Beutner, M. Lawler, P. Lobben, C–H arylation in the formation of a complex pyrrolopyridine, the commercial synthesis of the potent JAK2 inhibitor, BMS-911543, J. Org. Chem. 84 (2018) 4661–4669.
[19] S. Shirakami, Y. Nakajima, J. Maeda, H. Tominaga, H. Yamagishi, T. Hondo, M. Inami, H. Morio, T. Inoue, T. Mizutani, H. Ishioka, Condensed pyrrolopyridine derivative, U.S. Patent Application 13/264 (2012) 8.
[20] L.X. Wang, X. Liu, S. Xu, Q. Tang, Y. Duan, Z. Xiao, J. Zhi, L. Jiang, P. Zheng, W. Zhu, Discovery of novel pyrrolo-pyridine/pyrimidine derivatives bearing pyridazinone moiety as c-Met kinase inhibitors, Eur. J. Med. Chem. 141 (2017) 538–551.
[21] A.R. Blaazer, J.H. Lange, M.A. van der Neut, A. Mulder, F.S. den Boon, T.R. Werkman, C.G. Kruse, W.J. Wadman, Novel indole and azaindole (pyrrolopyridine) cannabinoid (CB) receptor agonists: design, synthesis, structure–activity relationships, physicochemical properties and biological activity, Eur. J. Med. Chem. 46 (2011) 5086–5098.
[22] E. Forcellini, S. Boutin, C.A. Lefebvre, E.E. Shayhidin, M.C. Boulanger, G. Rhéaume, X. Barbeau, P. Lagüe, P. Mathieu, J.F. Paquin, Synthesis and biological evaluation of novel quinazoline-4-piperidinesulfamide derivatives as inhibitors of NPP1, Eur. J. Med. Chem. 147 (2018) 130–149.
[23] S. Ullah, M.I. El-Gamal, S. Zaib, H.S. Anbar, S.O. Zaraei, R.M. Sbenati, J. Pelletier, J. Sévigny, C.H. Oh, J. Iqbal, Synthesis, biological evaluation, and docking studies of new pyrazole-based thiourea and sulfonamide derivatives as inhibitors of nucleotide pyrophosphatase/phosphodiesterase, Bioorg. Chem. 99 (2020) 103783.
[24] W.J. Ehlhardt, Metabolism and disposition of the anticancer agent sulofenur in mouse, rat, monkey, and human, Drug Metab. Dispos. 19 (1991) 370–375.
[25] W.J. Ehlhardt, H.R. Sullivan, P.G. Wood, J.M. Woodland, M. Hamilton, C. Hamilton, D. Cornpropst, G.B. Grindey, J.F. Worzalla, J.R. Bewley, G.C. Todd, J.J. Howbert, Pharmacokinetics of the anticancer agent sulofenur in mice, rats, monkeys, and dogs, J. Pharm. Sci. 82 (1993) 683–688.
[26] M.A. El-Sherbeny, A.A.-M. Abdel-Aziz, M.A. Ahmed, Synthesis and antitumor evaluation of novel diarylsulfonylurea derivatives: molecular modeling applications, Eur. J. Med. Chem. 45 (2010) 689–697.
[27] R.G. Boyle, S. Travers, *N*-Oxide-containing compounds as hERG inhibitors and their preparation, pharmaceutical compositions and use in the treatment of diseases, WO (2008) 2008139152.
[28] C.C. Cheng, C.P. Chang, W.S. Yu, F.T. Hung, Y.I. Liu, G.R. Wu, P.T. Chou, Comprehensive studies on dual excitation behavior of double proton versus charge transfer in 4-(*N*-substituted amino)-1H-pyrrolo [2, 3-b] pyridines, J. Phys. Chem. 107 (2003) 1459–1471.
[29] S.I. Belli, J.W. Goding, Biochemical characterization of human PC-1, an enzyme possessing alkaline phosphodiesterase I and nucleotide pyrophosphatase activities, Eur. J. Biochem. 226 (1994) 433–443.
[30] A.H. Abdelazeem, A.M. Gouda, H.A. Omar, M.F. Tolba, Design, synthesis and biological evaluation of novel dephenylthiazole-based cyclooxygenase inhibitors as potential anticancer agents, Bioorg. Chem. 57 (2014) 132–141.
[31] R.U. Takahashi, H. Miyazaki, F. Takeshita, Y. Yamamoto, K. Minoura, M. Ono, M. Kodaira, K. Tamura, M. Mori, T. Ochiya, Loss of microRNA-27b contributes to breast cancer stem cell generation by activating ENPP1, Nat. Commun. 6 (2015) 1–15.
[32] M. Kawaguchi, X. Han, T. Hisada, S. Nishikawa, K. Kano, N. Ieda, J. Aoki, T. Toyama, H. Nakagawa, Development of an ENPP1 fluorescence probe for inhibitor screening, cellular Imaging, and prognostic assessment of malignant breast cancer, J. Med. Chem. 62 (2019) 9254–9269.
[33] W.M. Lau, M. Doucet, R. Stadel, D. Huang, K.L. Weber, S.L. Kominsky, Enpp1: a potential facilitator of breast cancer bone metastasis, PloS One 8 (2013) 66752.
[34] I. Aerts, J.J. Martin, P.P. De Deyn, C. Van Ginniken, X. Van Ostade, M. Kockx, G. Dua, H. Slegers, The expression of ecto-nucleotide pyrophosphatase/phosphodiesterase 1 (E-NPP1) is correlated with astrocytic tumor grade, Clin. Neurol. Neurosurg. 113 (2011) 224–229.
[35] Y. Yano, Y. Hayashi, K. Sano, H. Shinmaru, Y. Kuroda, H. Yokozaki, S. Yoon, M. Kasuga, Expression and localization of ecto-nucleotide pyrophosphatase/phosphodiesterase I-3 (E-NPP3/CD203c/PD-Iβ/B10/gp130RB13-6) in human colon carcinoma, Int. J. Mol. Med. 12 (2003) 763–766.
[36] Y. Yano, Y. Hayashi, K. Sano, H. Nagano, M. Nakaji, Y. Seo, T. Ninomiya, S. Yoon, H. Yokozaki, M. Kasuga, Expression and localization of ecto-nucleotide pyrophosphatase/phosphodiesterase I-1 (E-NPP1/PC-1) and-3 (E-NPP3/CD203c/PD-Iβ/B10/gp130RB13-6) in inflammatory and neoplastic bile duct diseases, Cancer lett 207 (2004) 139–147.
[37] J. Baird, G. Dietsch, V. Florio, M. Gallatin, C. Knox, J. Odingo, M. Crittenden, Gough, M.J. MV-626, A Potent and Selective Inhibitor of ENPP1 Enhances STING Activation and Augments T-Cell Mediated Anti-tumor Activity in Vivo, (2018).
[38] J.A. Carozza, V. Bohnert, K.C. Nguyen, G. Skariah, K.E. Shaw, J.A. Brown, M. Rafat, R. von Eyben, E.E. Graves, J.S. Glenn, M. Smith, L. Li, Extracellular 2'3'-cGAMP is an immunotransmitter produced by cancer cells and regulated by ENPP1, BioRxiv (2019) 539312.
[39] L. Li, Q. Yin, P. Kuss, Z. Maliga, J.L. Millan, H. Wu, T.J. Mitchison, Hydrolysis of 2′ 3′-cGAMP by ENPP1 and design of nonhydrolyzable analogs, Nat. Chem. Biol. 10 (2014) 1043–1048.
[40] I. Belzer, I. Friedberg, ATP-resistant variants of transformed mouse fibroblasts, J. Cell. Physiol. 140 (1989) 524–529.
[41] T. Mure, K. Sano, T. Kitagawa, Modulation of membrane permeability, cell proliferation and cytotoxicity of antitumor agents by external ATP in mouse tumor cells, Jpn. J. Canc. Res. 83 (1992) 121–126.
[42] L.M. Zheng, A. Zychlinsky, C.C. Liu, D.M. Ojcius, J.D.E. Young, Extracellular ATP as a trigger for apoptosis or programmed cell death, J. Cell Biol. 112 (1991) 279–288.
[43] A. Filippini, R.E. Taffs, T. Agui, M.V. Sitkovsky, Ecto-ATPase activity in cytolytic

T-lymphocytes. Protection from the cytolytic effects of extracellular ATP, J. Biol. Chem. 265 (1990) 334–340.
[44] B. Spungin, I. Friedberg, Growth inhibition of breast cancer cells induced by exogenous ATP, J. Cell. Physiol. 157 (1993) 502–508.
[45] E. Rapaport, Experimental cancer therapy in mice by adenine nucleotides, Eur. J. Canc. 24 (1988) 1491–1497.
[46] W.G. Fang, F. Pirnia, Y.J. Bang, C.E. Myers, T.B. Trepel, P2-purinergic receptor agonists inhibit the growth of androgen-independent prostate carcinoma cells, J. Clin. Invest. 89 (1992) 191–196.
[47] G.G. Yegutkin, F. Marttila-Ichihara, M. Karikoski, J. Niemel∈a, J.P. Laurila, K. Elima, S. Jalkanen, M. Salmi, Altered purinergic signaling in CD73-deficient mice inhibits tumor progression, Eur. J. Immunol. 41 (2011) 1231–1241.
[48] H. Ahmad, S. Ullah, F. Rahman, A. Saeed, J. Pelletier, J. Sévigny, A. Hassan, J. Iqbal, Synthesis of biphenyl oxazole derivatives via Suzuki coupling and biological evaluations as nucleotide pyrophosphatase/phosphodiesterase-1 and-3 inhibitors, Eur. J. Med. Chem. 208 (2020) 112759.
[49] D. Sola, L. Rossi, G.P.C. Schianca, P. Maffioli, M. Bigliocca, R. Mella, F. Corliano, G.P. Fra, E. Bartoli, G. Derosa, Sulfonylureas and their use in clinical practice, Arch. Med. Sci. 11 (2015) 840–848.
[50] A. Douros, H. Yin, O.H.Y. Yu, K.B. Filion, L. Azoulay, S. Suissa, Pharmacologic differences of sulfonylureas and the risk of adverse cardiovascular and hypoglycemic events, Diabetes Care 40 (2017) 1506–1513.
[51] S.A. Levesque, E.G. Lavoie, J. Lecka, F. Bigonnesse, J. Sévigny, Specificity of the ecto-ATPase inhibitor ARL 67156 on major ecto-nucleotidases, Br. J. Pharmacol. 152 (2007) 141–150.
[52] M.M. Bradford, A rapid and sensitive method for the quantitation of microgram quantities of protein utilizing the principle of protein-dye binding, Anal. Biochem. 72 (1976) 248–254.
[53] E. Ausekle, S.A. Ejaz, S.U. Khan, P. Ehlers, A. Villinger, J. Lecka, J. Sévigny, J. Iqbal, P. Langer, New one-pot synthesis of *N*-fused isoquinoline derivatives by palladium-catalyzed C–H arylation: potent inhibitors of nucleotide pyrophosphatase-1 and-3, Org, Biomol. Chem. 14 (2016) 11402–11414.
[54] A.H. Abdelazeem, A.M. Gouda, H.A. Omar, M.F. Tolba, Design, synthesis and biological evaluation of novel dephenylthiazole-based cyclooxygenase inhibitors as potential anticancer agents, Bioorg. Chem. 57 (2014) 132–141.
[55] K. Kato, H. Nishimasu, S. Okudaira, E. Mihara, R. Ishitani, J. Takagi, J. Aoki, O. Nureki, Crystal structure of NPP1, an extracellular glycoprotein involved in bone mineralization and insulin signaling, Proc. Natl. Acad. Sci. U.S.A. 109 (2012) 16876–16881.
[56] A. Gorelik, A. Randriamihaja, K. Illes, B. Nagar, Structural basis for nucleotide recognition by the ectoenzyme CD 203c, FEBS J. 285 (2018) 2481–2494.
[57] MOE Molecular Operating Environment Version, 0901. Chemical Computing Group, (CCG), 2014. http://www.chemcomp.com/MOE Molecular_Operating_Environment.htm.
[58] LeadIT Version 2.3.2, BioSolveIT GmbH, Sankt Augustin, Germany, 2017. http://www.biosolveit.de/LeadIT.
[59] Dassault Systmes BIOVIA, Discovery Studio Modeling Environment, Release, Dassault Systemes, San Diego, 2017, 2016.